Shock Waves (2017) 27:431–439
DOI 10.1007/s00193-016-0701-9

ORIGINAL ARTICLE

Mechanism of formation of reflection configurations over concave surfaces

I. V. Krassovskaya[1] · **M. K. Berezkina**[1]

Received: 17 September 2014 / Revised: 13 October 2016 / Accepted: 5 November 2016 / Published online: 24 November 2016

Abstract Shock wave reflection from concave cylindrical and elliptical wedges is numerically studied. The model of a polyhedron inscribed into a circular cylinder is used to elucidate the mechanism of formation of reflection configurations in unsteady flows. This numerical simulation gives a clear indication of how the initial incident shock wave "receives information" from the reflecting surface. Flow features resulting from shock reflection off smooth, concave wedges are considered for different shapes of the reflecting surface. It is found that the evolution of the shock wave reflection configuration is determined by the shape of the reflecting wedge. It is shown that the Mach to regular reflection (MR → RR) transition angles are different for different reflecting surfaces with the same incident shock Mach number.

Keywords Unsteady reflection · Inscribed polyhedron · Concave cylindrical wedge · Concave elliptical wedge · Mechanism of formation of shock reflection configuration · Numerical simulation

1 Introduction

In spite of the practical importance of the problem of unsteady shock wave reflection over curved surfaces, attention has traditionally been paid to the investigation of the simplest curvilinear surfaces—concave and convex cylindrical walls [1–4]. The unsteady reflection process has been described as a series of consequential changes of reflection configurations depending on an incident shock Mach number M and a local slope angle [5]. In the case of reflection off a concave cylindrical surface with zero initial angle, these configurations are: von Neumann reflection (vNR) → Mach reflection (MR) → inverse Mach reflection (InMR) → transitioned regular reflection (TRR). In [3], it was shown that the reflection configurations obtained in an unsteady flow differ noticeably from the configurations obtained at pseudo-steady shock reflection for the same incident shock Mach numbers and slope angles. The complex flow features arising from the interaction of a shock wave with a concave cylindrical wall were determined in [6]. The study has indicated that the description of the unsteady reflection process mentioned above is imprecise. The reflection configurations arising in the course of the unsteady reflection process are not the ideal ones on which the classical von Neumann theory is based. That has been clearly demonstrated in [7] by comparing the experimental data with the calculation results in the von Neumann theory.

Figure 1 presents two three-shock configurations. The shadowgraph image from experimental results illustrates a Mach configuration over a cylindrical concave arc of a 100 mm radius with an incident shock Mach number $M = 2.5$ in CO_2 (heat capacities ratio $\gamma = 1.29$) at $t = 80\,\mu$s. The tangent line to the concave surface in the Mach stem foot is inclined at $\beta = 36°$. Using the elementary three-shock theory, we calculated the ideal Mach configuration for $M = 2.5$, $\beta = 36°$, and $\gamma = 1.29$. White lines show this configuration superimposed over the experimental image; φ is the angle between the incident and the reflected shock waves, ψ is the angle between the reflected shock wave and the slipstream, and θ is the angle between the slipstream and the Mach stem. Knowing the Mach stem length and the angle α between the incident shock wave and trajectory of the triple point of the

Communicated by A. Sasoh.

✉ I. V. Krassovskaya
i.kras@mail.ioffe.ru

[1] Ioffe Institute, Politekhnicheskaya ul. 26, St. Petersburg 194021, Russia

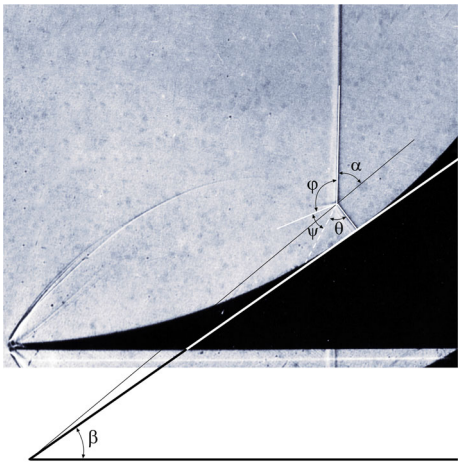

Fig. 1 Mach reflection configuration with $M = 2.5$ and $\gamma = 1.29$. Experimental and calculation results

ideal Mach configuration, the location of the leading edge of the imaginary straight wedge can be reconstructed. The disagreement between the geometries and the locations of the leading edges of the experimental and calculated configurations is obvious. These data testify that three-shock configurations arising in unsteady reflection cannot be interpreted with the help of the von Neumann theory which is valid for pseudo-steady reflection. Unsteady shock wave reflection is a process much more complicated than a sequence of ideal shock-wave configurations corresponding to the local values of an incident shock Mach number and a wall angle.

To provide a better understanding of the physical mechanism of formation of reflection configurations over a concave cylindrical surface, various diagnostic approaches were proposed. Suzuki et al. [8] applied an approach with the method of multiple steps. A cylindrical reflecting surface was simulated by a step-like wedge. The surface of the step-like wedge was composed of multiple steps with constant height. The radius of curvature of the step-like wedge was equivalent to the radius of the cylindrical wedge. The experimental results of shock wave reflection over a concave step-like wedge contribute to better understanding of the reflected shock formation, but they do not illustrate the Mach stem formation and evolution of the three-shock configuration. It appears that the step-like wedge model does not provide a sufficiently accurate simulation of a cylindrical surface.

Skews and Kleine [9] used the method based on tracking very weak perturbations generated in the post-shock flow. The diagnostic technique was used in conjunction with high-speed time-resolved photography. The data obtained for the Mach number 1.35 and a 64-mm-radius cylinder demonstrated that the surface curvature results in a series of compression waves spreading across the incident shock wave. The compression causes the incident wave to bend smoothly forward increasing in strength towards the surface. Merging of compression waves results in a kink on the incident shock front and subsequently, in the formation of a reflected shock and a Mach stem. However, the Mach stem has to play the role of the incident shock. This circumstance should also be considered when investigating the reflection process. The results of this work suggest that there is a need to continue the investigation of shock reflection over a cylindrical surface, because only a few features of the complex flow structure have been revealed.

The objective of this paper is to elucidate the mechanism of formation of various configurations that arise, while a shock wave propagates along smooth concave surfaces of different shapes. For better understanding of the process, numerical calculation of a shock reflection off an inscribed polyhedron surface has been carried out.

2 Numerical method

For computations of unsteady inviscid flows, a solver [10] intended for integration of the Euler equations has been used. The code has successfully been applied to a variety of gasdynamic problems. It is based on an explicit quasi-monotonous scheme of Godunov-type with a second-order accuracy both in space and time. The use of unstructured grids with the dynamical adaptation to the flow features (shock waves, slip-streams, etc.) allows detailed information about the evolution of complex shock-wave structures to be obtained. To test the numerical set-up, a set of computations using different grid refinement levels was performed for the reflection of the shock waves from a concave cylindrical surface. The computational results are shown in Fig. 2. The comparison between the results demonstrates good grid convergence in terms of shock intensities and gas parameters. The only grid-dependent features are the relative widths of shock waves and shear layers. The slight disagreement in shear layer instability at different grid refinement levels can also be seen. Since the main concern of this contribution is to elucidate the mechanism of formation of unsteady shock wave reflection patterns, it was concluded that the numerical simulation using the grid refinement levels equal to seven is suitable for such study. More details regarding the numerical method and code can be found in [11].

3 Results and discussion

3.1 Shock wave reflection off a polyhedron inscribed in a cylinder

To elucidate the mechanism of formation of the reflection configuration, we performed a numerical simulation of a shock wave reflection off a multi-faceted concave wedge.

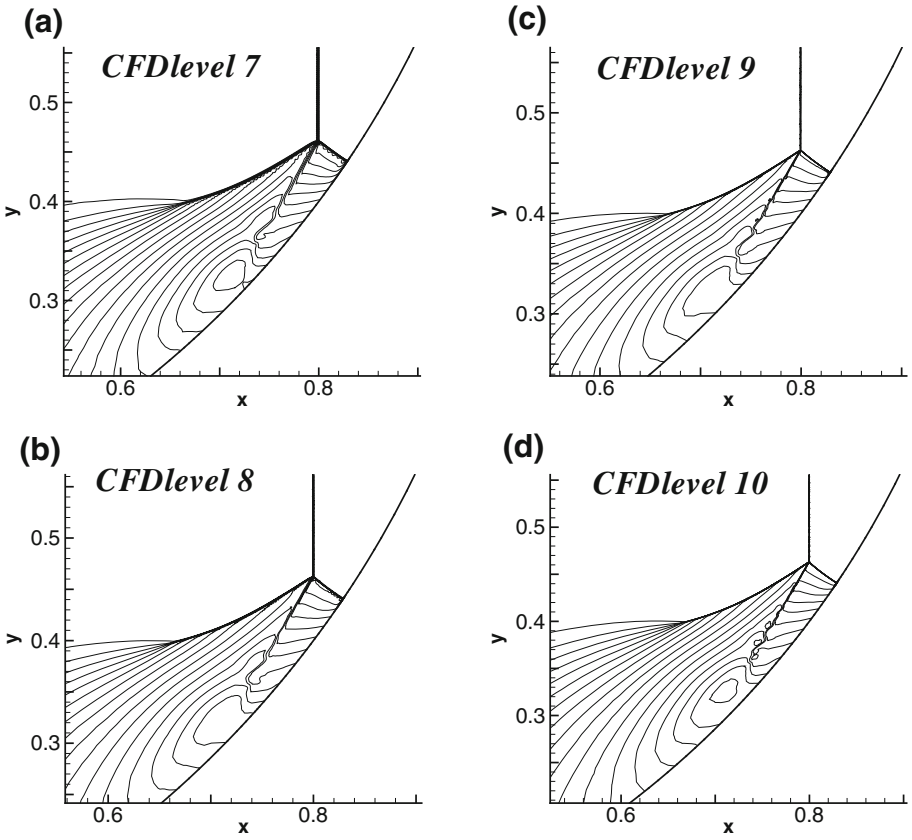

Fig. 2 Comparison of the simulation of the reflection of a shock wave from a concave cylindrical surface using different grid refinement levels. Density contours. $M = 2.5$, $\gamma = 1.29$

A polyhedron inscribed in a cylinder of radius R can be successfully used, because the cylindrical surface is the limit of a polyhedron with $n \to \infty$ (where n is the number of facets of the polyhedron). The computation was performed for $M = 2.5$, $\gamma = 1.29$, and for 1/4 of tetraicosagon (24 facets) as the reflecting surface. All sizes are related to R; time scale is the time that it takes the incident shock wave to cover the distance R. The numerical density contours for different instances are presented in Fig. 3. Figure 3a corresponds to the instant $t = 0.200$, at which the incident shock wave reflects from the first facet as a vNR. The incident wave and the Mach stem constitute a smooth curve without a discontinuity in slope; the reflected signal is a compression wave. Note that usually a vNR is referred to as the pattern obtained for weak shocks and small wall angles. The given configuration is obtained for $\beta = 7.5°$ and $M = 2.5$, i.e., for a strong shock wave with a supersonic flow behind its front. An attached shock wave is formed over the leading edge of the first facet.

At $t = 0.535$ (Fig. 3b), the initial incident shock wave is located over the third facet of the polyhedron. Three triple points can be seen. The triple point T_1^* was obtained when the initial shock wave reflected from the first facet. The Mach reflection with the point T_2 was obtained when the Mach stem reflected from the second wedge, and the Mach configuration with the point T_3 arose when the Mach stem of the latter shock configuration reflected from the third facet. Here and elsewhere, an asterisk is used to mark the triple point located on the initial incident shock wave. Occurrence of the three triple points testifies that at $t = 0.535$, the disturbances from the second and third facets have not yet reached the initial incident wave. The type of reflection configuration can be referred to as a vNR with the additional triple points on the Mach stem.

As the initial incident shock wave propagates, two processes are responsible for the formation of the shock-wave configurations. These are the successive collisions of the triple points leading to the formation of new three-shock configurations and the reflections of the newly formed Mach stem from the succeeding facets of the polyhedron. The three-shock configuration with the point T_4^* which was formed after collisions of the points T_1^*, T_2, and T_3 is presented in Fig. 3c ($t = 0.700$). The triple point T_4 arose as a result of reflection of the new Mach stem from the fourth facet. The reflection configuration with the point T_4^* is a MR with the additional triple point on the Mach stem and the triple point on the reflected wave.

Eventually, multiple collisions of the triple points result in the formation of a single three-shock configuration on the fifth facet of the polyhedron (Fig. 3d, $t = 0.900$). The reflection configuration has a straight Mach stem, but there are some additional triple points on the reflected wave. That is an InMR configuration, because the triple point T_5^* moves towards the fifth facet and collides with it. After the termi-

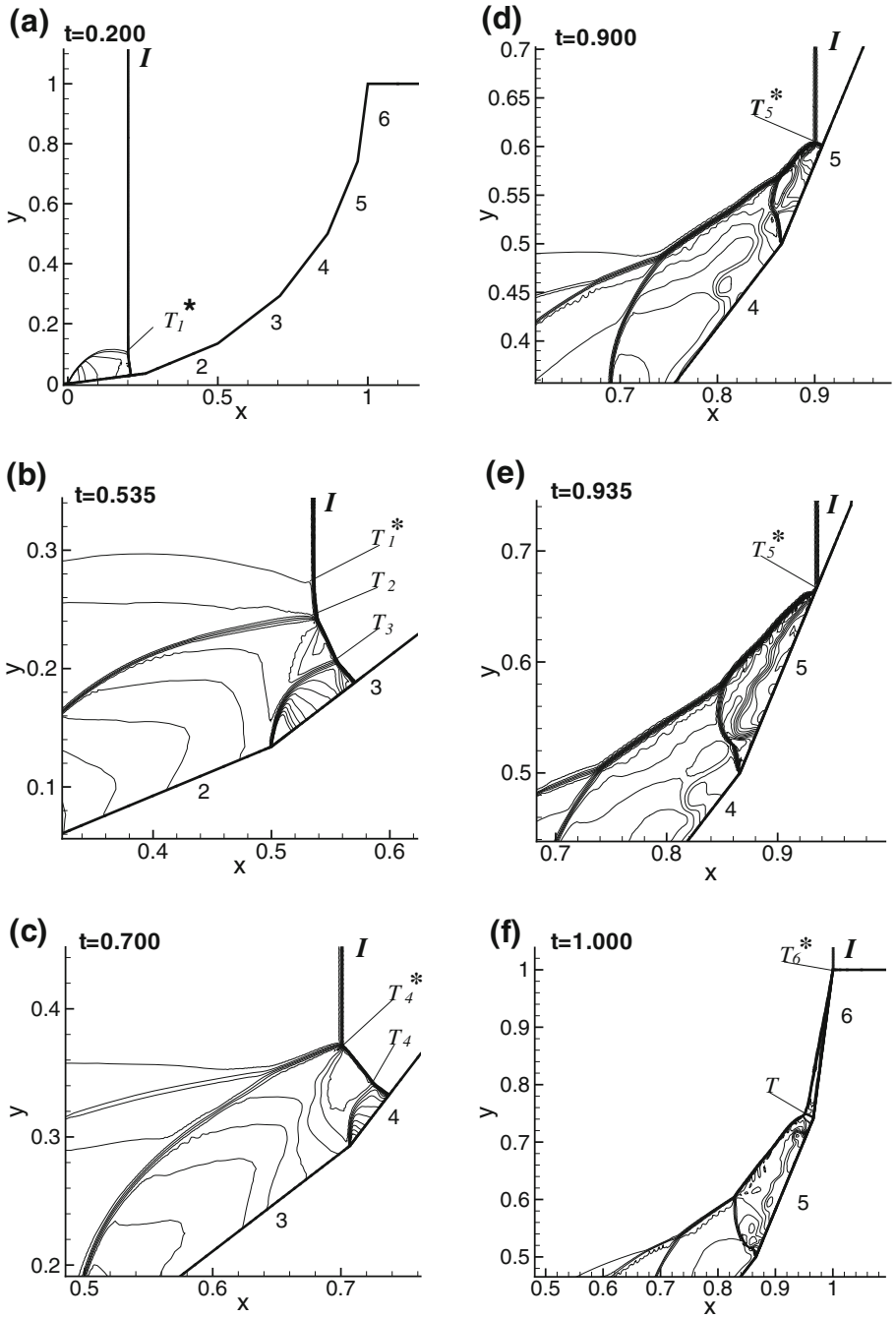

Fig. 3 Numerical simulation of $M = 2.5$ shock wave reflecting off the tetraicosagon ramp. Density contours (sequential shock wave patterns)

nation of the InMR, the structure known as a transitioned regular reflection (TRR) [1] arises on the fifth facet (Fig. 3e). The major part of the shock pattern is a regular reflection (RR) of the initial incident shock wave with the reflection point T_5^*. In addition, a new triple point T is formed on the reflected wave. The structure is clearly seen in the next Fig. 3f ($t = 1.0$). The RR on the fifth facet changes into the RR with the reflection point T_6^* on the sixth facet. The additional configuration is located just ahead of the leading edge of the last facet, and details of the configuration are clearly seen. Apparently, the additional three-shock configuration results from the interaction of the reflected wave of the RR with the reflected wave of the MR. The resulting wave of the additional configuration is perpendicular to the fifth facet and will subsequently reflect off the sixth facet. Note that the TRR structure was first reported in [3] where the results of an investigation of a shock wave reflection from a concave cylindrical ramp were presented. The flow field over the whole area at $t = 1.0$ is presented in Fig. 4. The picture illustrates very clearly how the reflected wave is formed.

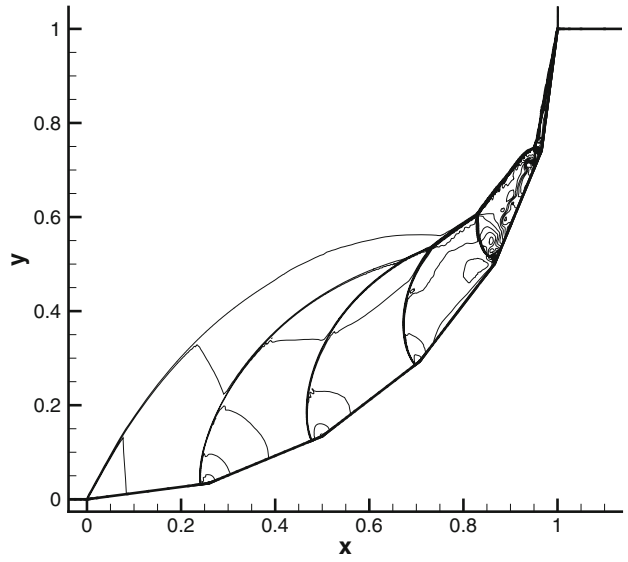

Fig. 4 Whole flow field around the tetraicosagon ramp at $t = 1.0$. Density contours

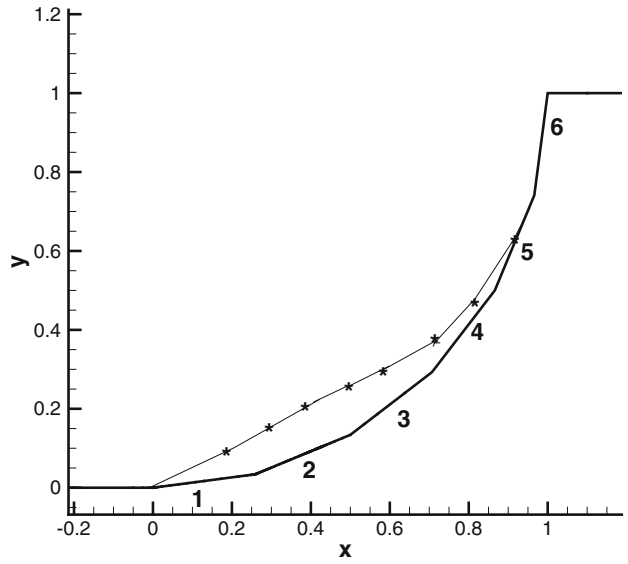

Fig. 5 Trajectory of the main triple point T^*

Computational results suggest that the reflection process follows the following sequence of events: vNR → MR → InMR → TRR. Figure 5 shows the trajectory of the main triple point (marked with an asterisk) over the reflecting multi-faceted wedge. The distance between the triple point and the surface increases from 0.0 at the leading edge of the reflecting surface to a maximum after which it decreases until it vanishes. The non-monotone run of the curve of the trajectory of the main triple point is caused by the fact that as the resulting triple points merge, a new three-shock configuration is formed. The triple point of the configuration can move either away from the surface or towards the reflecting surface.

Considering the mechanism of formation of reflection configurations, we can suppose that the behavior of the triple point depends strongly on the length and wall angle of each facet of the polyhedron. It means that in the case of a concave smooth reflecting wall, the shape of the reflecting surface defines the evolution of the shock wave reflection configuration.

3.2 Shock wave reflection off smooth concave reflecting walls

The model of a polyhedron inscribed in a cylinder provides a clear understanding of the mechanism of formation of shock-wave reflection configurations in unsteady flows. Since a smooth cylindrical surface is the limit of a polyhedron where the number of facets tends to infinity, it is clear that the foot of a shock wave moving along a smooth surface will generate continuous perturbations. These perturbations will be continuously passed on to the incident wave causing the formation of reflection configurations. Apparently, the reflection configurations will have curved reflected waves and Mach stems, and a gradient field behind them.

To consider the influence of the curvature of the reflecting wall on the dynamics of the reflection process, a numerical simulation of a shock wave interacting with various smooth concave ramps with a zero initial ramp angle was performed. Computations were made for $M = 2.5$ and $\gamma = 1.29$. A total of four reflecting surfaces were tested. Table 1 lists the considered variants of the reflecting ramps. Variants 2 and 3 are piecewise-smooth surfaces consisting of two cylindrical segments. Below, all sizes are related to R—radius of the circular cylinder of var. 1. Time scale is the time that it takes the incident shock wave to cover the distance R. For var. 2, the dimensionless radii of the first and second segments are equal to 1 and 3, respectively. For var. 3, these radii are equal to 1 and 1/3, respectively. At $x = 0.6$, $\mathrm{d}y/\mathrm{d}x$ is the same for variants 1–3 . Figure 6 shows the shapes of the reflecting ramps.

Table 1 Reflecting surfaces

Var.	Surface	Determining equation
1	Circular cylinder	$x^2 + (y-1)^2 = R^2$
2	Compound surface	$x^2 + (y-1)^2 = R^2, x \le 0.6$; $(x+1.2)^2 + (y-2.6)^2 = 9R^2$, $x > 0.6$
3	Compound surface	$x^2 + (y-1)^2 = R^2, x \le 0.6$; $(x-0.4)^2 + (y-0.467)^2 = R^2/9$, $x > 0.6$
4	Circular ellipse	$(x/4)^2 + (y-1)^2 = 1$

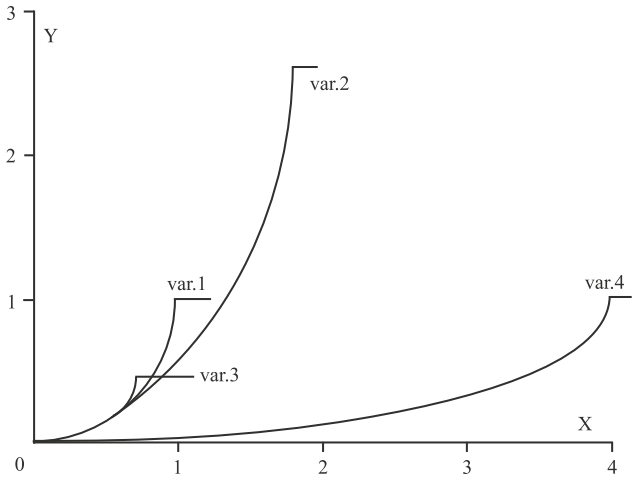

Fig. 6 Shapes of the reflecting surfaces

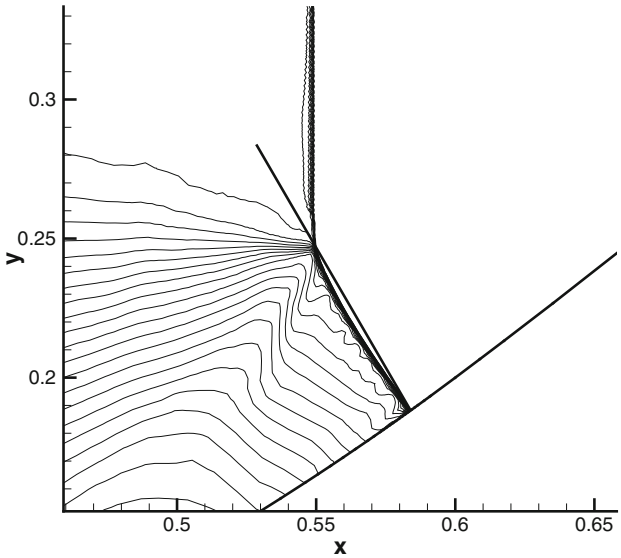

Fig. 7 Mach reflection configuration obtained from reflection of a shock wave off a concave cylindrical ramp at $t = 0.55$. Density contours

For var. 1–3, computational results as density contours are given in Figs. 7, 8, 9, 10. Because variants 1–3 have the same cylindrical segment $0.0 < x < 0.6$, the first stage of the reflection process is also the same. Figure 7 shows a Mach configuration with curved Mach stem, which is formed at $t = 0.55$ (the straight line connecting two extremities of the Mach stem is drawn to demonstrate its curvature). The first stage of the reflection process ends at $t \simeq 0.575$, when the foot of the Mach stem reaches the point ($x = 0.6$, $y = 0.2$). At this moment, the Mach configuration is the same for all variants. Starting from this moment, the MR configuration will propagate along smooth cylindrical arcs of different radii. Flowfield histories are shown in Fig. 8. For each variant, density contours are presented for two locations of an incident shock wave: when an incident shock wave is in the point $x = 0.6$ and when it is in the vertex of the reflecting ramp.

As flow patterns in Fig. 8 demonstrate, transition from MR to TRR occurs for all considered reflecting walls. T is the additional triple point on the reflected shock wave. An enlarged fragment of Fig. 8b showing the flowfield in the vicinity of the point T is presented in Fig. 9. This structure is formed after termination of an InMR. The initial incident shock wave reflects over surface as a RR. r is a reflected shock. However, the elements of a InMR still exist in the flow. These are the reflected shock wave r_M and shear layer S_M. Interaction between reflected shocks r and r_M results in formation of the additional three-shock configuration. T is the triple point, m is the resulting shock, and S is the shear layer. The region with high values of density and pressure is behind the resulting shock wave of the additional three-shock configuration. It decelerates the motion of gas along the reflecting surface. The nature of this additional configuration is the same for all the cases under consideration. To examine that structure, its formation, and evolution, further research must be carried out in the future. While the transition from Mach to regular reflection is beyond the scope of this work, the assessment of the transition angle values was performed. The transition angle β_{tr} (β is a local wall angle) was defined as an average value between two local angles.

One angle is determined according to the flow picture where the last MR is obtained. The other angle is determined according to the flow picture, where the first appearance of the RR is obtained. For variants 1–3, the following transition angles were obtained: $\beta^1_{tr} = 68° \pm 3°$, $\beta^2_{tr} = 66° \pm 4°$, and $\beta^3_{tr} = 83° \pm 7°$. The detachment (det) and mechanical equilibrium (me) criteria have been suggested by von Neumann (see [1,2]) for the transition between RR and MR pseudo-steady configurations. For $M = 2.5$ and $\gamma = 1.29$, $\beta_{det} = 48.94°$, $\beta_{me} = 58.72°$. The transition between irregular and regular unsteady reflection configurations occurs at angles greater than the angle corresponding to the mechanical equilibrium criterion. It should be noted that the values obtained in the present work are a crude assessment of the transition angles. Since at $t \simeq 0.575$, the same MR was formed for all variants; at the second stage of the reflection process, an important role will be played by the ratio of the length of the Mach stem of the MR to the radius of the second segment of the reflecting arc. The larger the ratio, the greater is the transition angle.

In case of var. 3, apart from the additional triple point, the reflected shock wave features the kink k (Fig. 8c). To elucidate the reason for the occurrence of the kink, it is useful to consider the reflection process over the second segment in more detail (Fig. 10). The initial shock wave reflection off the first segment leads to the formation of the MR configuration. The length of the Mach stem of this configuration with respect to the radius of the second segment is three times

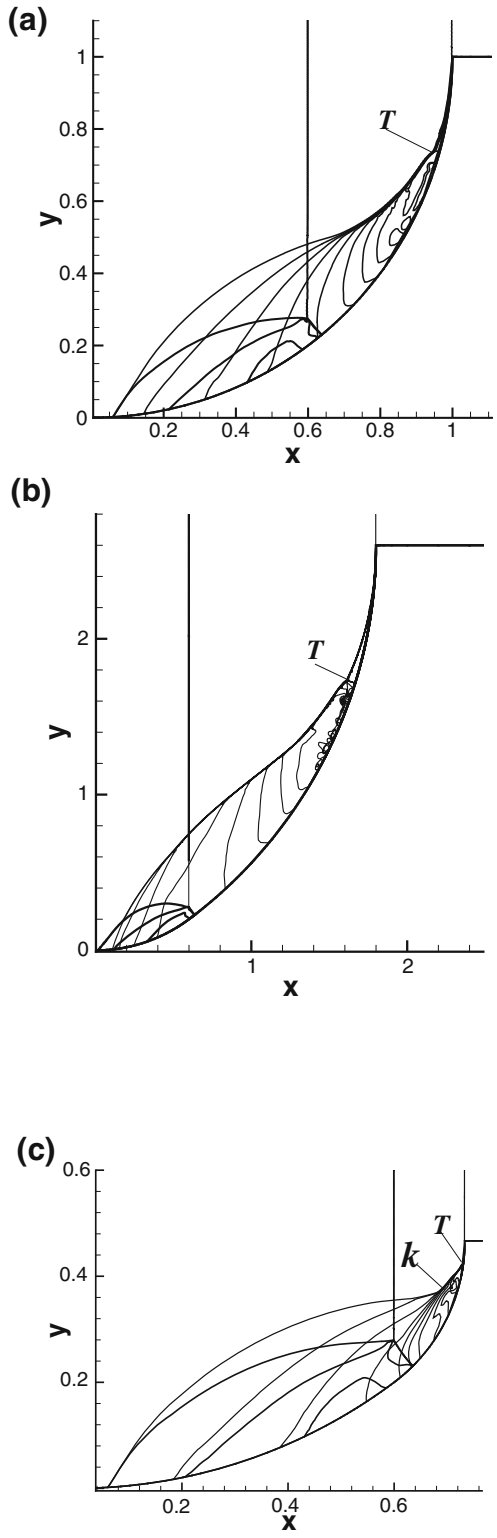

Fig. 8 Numerical simulation of $M = 2.5$ shock reflecting off different concave smooth ramps. Density contours. **a** Variant 1, **b** variant 2, **c** variant 3

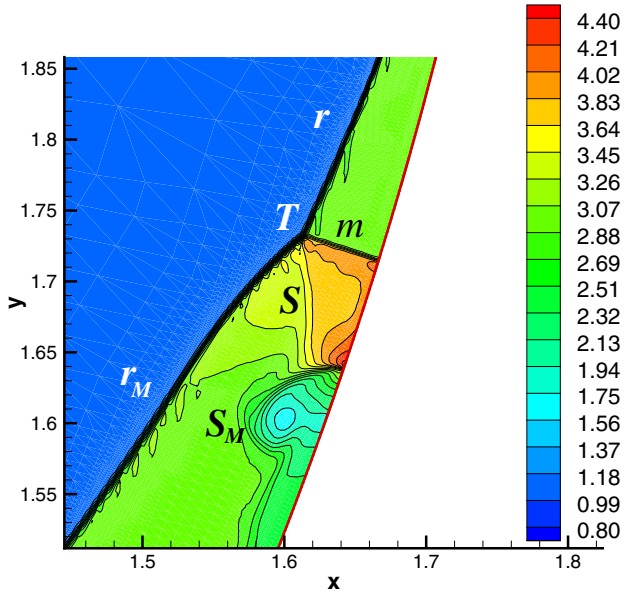

Fig. 9 Enlarged fragment of Fig. 8b. The flowfield in the vicinity of the point T. Density is indicated by *color* and *lines*

greater than the same length with respect to the radius of the first segment. For this reason, for some time, the triple point T^* on the incident wave is not subjected to the process of the Mach stem reflection off the second segment (Fig. 10a). The process of the reflection of the Mach stem (it plays the role of an incident shock) from the second segment resembles most closely the process of the reflection of the initial shock wave off the first segment. However, by contrast to the reflection of the initial shock wave from the first reflecting segment, which is completed by the formation of the three-shock configuration, the reflection process of the Mach stem from the second segment leads to the formation of the von Neumann configuration type with the point T_M on the Mach stem and with not a reflected shock wave but rather a strong reflected compression wave. Eventually, merging of the triple point T^* and point T_M (Fig. 10b) results in the formation of a new three-shock configuration. Since the reflected compression wave emanating from the point T_M is rather strong, the kink k occurs on the resulting reflected shock wave of the main Mach configuration (Fig. 10c). It is known that interaction of a planar shock wave with a wedge is a combination of two sub-processes: shock wave reflection and an incident shock-induced flow deflection around the compressive wedge [13]. Comprehensive analysis of shock wave reflection in pseudo-steady flows was offered in [12]. Attention should be given to the fact that, in contrast to a Transitional Mach reflection (TMR) and a Double Mach reflection (DMR), where the additional kink (or the triple point) is the result of the combination

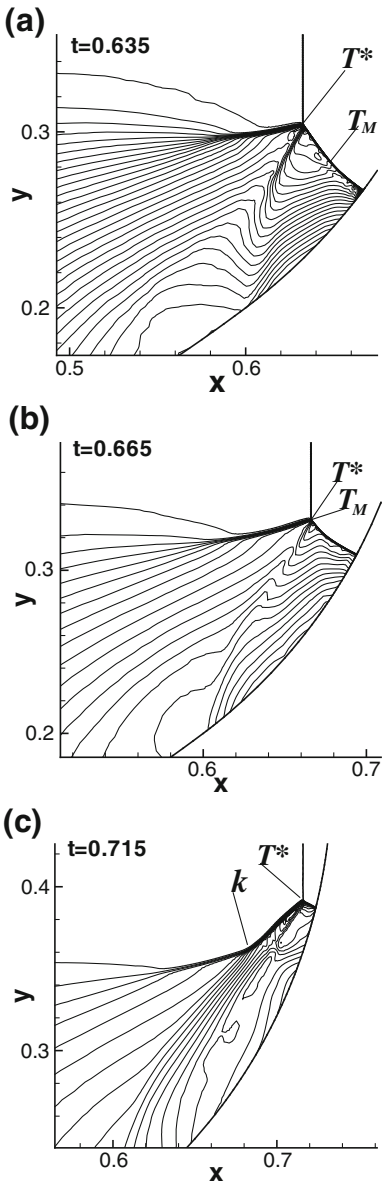

Fig. 10 Formation of the reflected shock wave for var. 3. Density contours

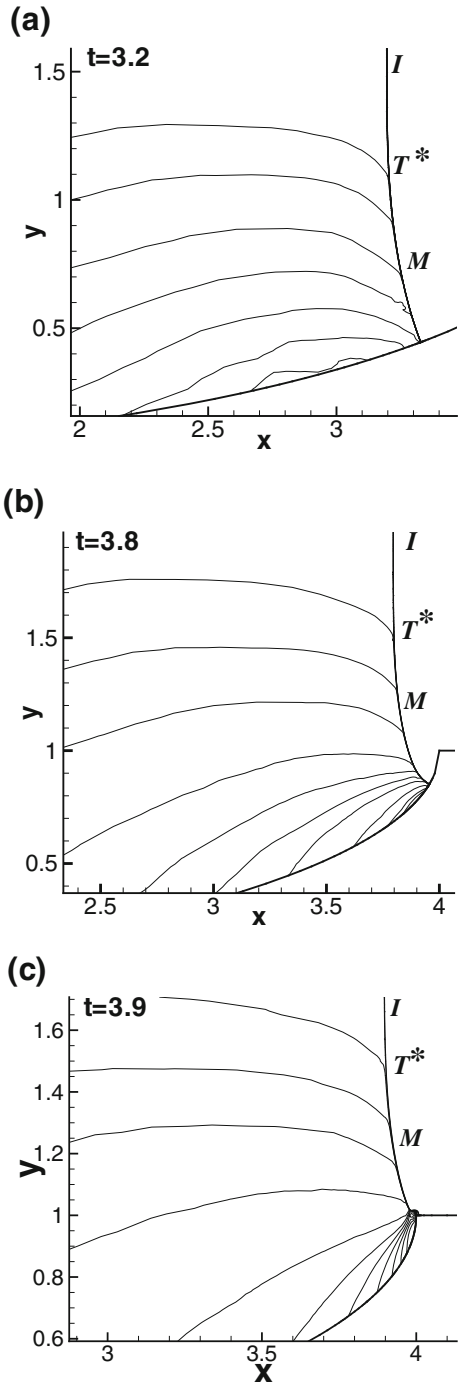

Fig. 11 Numerical simulation of $M = 2.5$ shock wave reflecting off the concave elliptical wall. Density contours

of two sub-processes: the shock reflection and the incident shock-induced flow deflection [12]; in the given case, the occurrence of the kink on the reflected wave is the result of changing the curvature of the reflecting surface. Analysis of the influence of an incident shock-induced flow deflection on shock wave reflection in unsteady flows is much more difficult than in pseudo-steady flows. In the case under consideration, the flow deflection processes as well as the shock reflection processes are different for var. 1–3. As shown in Fig. 8, the boundary of the perturbed flowfield represented by a shock wave along a half of the whole length for var. 1 (Fig. 8a), almost along the whole length for var. 2 (Fig. 8b), and it is represented by a sonic line along most of the length for var. 3 (Fig. 8c).

Numerical data of a shock wave reflection from a concave elliptical surface (var. 4) are presented in Fig. 11. The vNR configuration arises at the leading edge of the concave wedge. The triple point T^* divides the incident shock into undisturbed I and disturbed M (Mach stem) parts. For the given elliptical surface, the longer axis and the shorter axis of

the ellipse are related as 4:1. As the flow patterns show, the vNR configuration is maintained throughout the reflection process (Fig. 11). The point T^* is located much higher than the vertex of the reflecting wall and cannot make contact with the reflecting wall. In fact, not an initial incident shock wave, but the part of the Mach stem close to the wall—a curved shock wave with a nonlinear flow behind it—interacts with the surface. At $t = 3.9$, the curve part of the Mach stem diffracts over the vertex of the reflection surface (Fig. 11c). With regard to the initial incident shock wave, it should be noted that, as evidenced by this computation, during the whole reflection process of a shock wave off the given shape of the reflecting wall, the vNR type remains constant without transition to other reflection forms.

4 Concluding remarks

Numerical simulation of unsteady reflection of a planar shock wave from various concave reflecting ramps is performed. The model of a polyhedron inscribed in a cylinder as the reflecting surface provided understanding of the mechanism of formation of shock-wave configurations in unsteady flows. It is shown that configurations forming in unsteady flows are not determined by the incident shock Mach number M, the angle of the wedge, and the specific heat ratio, but result from complex sub-processes and cannot be described with the use of the von Neumann theory. The numerical data of a shock wave interaction with concave cylindrical and elliptical wedges have shown unambiguously that the evolution of reflection configurations is determined by the curvature of the concave reflecting wall. Transition angles between different kinds of unsteady reflection configurations depend on the shape of the reflecting wall and differ from transition angles obtained for pseudo-steady reflection.

References

1. Ben-Dor, G.: Shock Wave Reflection Phenomena, 2nd edn. Springer, Berlin (2007)
2. Ben-Dor, G., Igra, O., Elperin, T.: Handbook of Shock Waves. Academic Press, Dublin (2001)
3. Syshchikova, M.P., Semenov, A.N., Berezkina, M.K.: Shock wave reflection by a curved concave surface. Sov. Tech. Phys. Lett. **2**, 61–66 (1976)
4. Krassovskaya, I.V., Berezkina, M.K.: Reflection and diffraction of shock waves and shock wave configurations. In: 28th International Symposium on Shock Waves, Manchester, England, pp. 13–19 (2011)
5. Ben-Dor, G., Takayama, K.: Application of steady shock polars to unsteady shock wave reflections. AIAA J. **24**, 682–684 (1986)
6. Skews, B.W., Kleine, H.: Flow features resulting from shock wave impact on a cylindrical cavity. J. Fluid Mech. **580**, 481–493 (2007)
7. Berezkina, M.K., Krassovskaya, I.V.: Interaction of a planar shock wave with a cylindrical concave wedge. In: 20th International Symposium on Shock Interaction, Stock-holm, Sweden, pp. 5–8, 20–24 August (2012)
8. Suzuki, T., Adachi, T., Kobayashi, S.: Nonstationary shock reflection over nonstraight surfaces: an approach with a method of multiple steps. Shock Waves **7**, 55–62 (1997)
9. Skews, B.W., Kleine, H.: Anewdiagnostic approach to shock-wave reflection. In: 27th International Symposium on ShockWaves, St.Petersburg, Russia, pp. 314–319, 24 July (2009)
10. Fursenko, A.A., Sharov, D.M., Timofeev, E.V. and Voinovich, P.A.: An efficient unstructured Euler solver for transient shocked flows. Shock Waves @ Marsielle **I**, 371–376 (1995)
11. Drikakis, D., Ofengeim, D., Timofeev, E.V., Voinovich, P.A.: Computation of non-stationary shock-wave/cylinder interaction using adaptive-grid methods. J. Fluids Struct **11**(6), 665–692 (1997)
12. Semenov, A.N., Berezkina, M.K., Krassovskaya, I.V.: Classification of pseudo-steady shock wave reflection types. Shock Waves **22**(4), 307–316 (2012)
13. Law, C. K.: Diffraction of strong shock waves by sharp compressive corner. UTIAS Technical Note No. 150, Toronto, Canada (1970)